Frequency stabilization of a single mode terahertz quantum cascade laser to the kilohertz level

Andriy A. Danylov[1*], Thomas M. Goyette[1], Jerry Waldman[1], Michael J. Coulombe[1], Andrew J. Gatesman[1], Robert H. Giles[1], William D. Goodhue[2], Xifeng Qian[2], and William E. Nixon[3]

[1] *Submillimeter-Wave Technology Laboratory, Dept. of Physics and Applied Physics, University of Massachusetts Lowell, Lowell, Massachusetts, 01854, USA*

[2] *Photonics Center, Dept. of Physics and Applied Physics, University of Massachusetts Lowell, Lowell, Massachusetts, 01854, USA*

[3] *U.S. Army National Ground Intelligence Center, Charlottesville, Virginia 22911, USA*

[*] *Corresponding author: Andriy_Danylov@student.uml.edu*

Abstract: A simple analog locking circuit was shown to stabilize the beat signal between a 2.408 THz quantum cascade laser and a CH_2DOH THz CO_2 optically pumped molecular laser to 3-4 kHz (FWHM). This is approximately a tenth of the observed long-term (t ~ sec) linewidth of the optically pumped laser showing that the feedback loop corrects for much of the mechanical and acoustic-induced frequency jitter of the gas laser. The achieved stability should be sufficient to enable the use of THz quantum cascade lasers as transmitters in short-range coherent transceivers.

OCIS codes: (140.5965) Semiconductor lasers, quantum cascade; (140.3425) Laser stabilization; (300.3700) Linewidth; (040.2840) Heterodyne.

References and links

1. R. Köhler, A. Tredicucci, F. Beltram, H. E. Beere, E. H. Linfield, A. G. Davies, D. A. Ritchie, R. C. Iotti, and F. Rossi, "Terahertz semiconductor-heterostructure laser," Nature **417**, 156–159 (2002).
2. B. S. Williams, S. Kumar, Q. Hu, and J. L. Reno, "High-power terahertz quantum-cascade lasers," Electron. Lett. **42**, 89 (2006).
3. M. S. Vitiello, G. Scamarcio, V. Spagnolo, S. S. Dhillon, and C. Sirtori, "Terahertz quantum cascade lasers with large wall-plug efficiency," Appl. Phys. Lett. **90**, 191115 (2007).
4. C. Walther, M. Fischer, G. Scalari, R. Terazzi, N. Hoyler, and J. Faist, "Quantum cascade lasers operating from 1.2 to 1.6 THz," Appl. Phys. Lett. **91**, 131122 (2007).
5. M. A. Belkin, J. A. Fan, S. Hormoz, F. Capasso, S. P. Khanna, M. Lachab, A. G. Davies, and E. H. Linfield, "Terahertz quantum cascade lasers with copper metal-metal waveguides operating up to 178 K," Opt. Express **16**, 3242 (2008).
6. T. M. Goyette, J. C. Dickinson, J. Waldman, W. E. Nixon, and S. Carter, "Fully Polarimetric W-Band ISAR Imagery of Scale-Model Tactical Targets Using a 1.56 THz Compact Range," Proc. SPIE **4382**, 229-240, (2001).
7. J. Waldman, A. A. Danylov, T. M. Goyette, M. J. Coulombe, R. H. Giles, A. J. Gatesman, W. D. Goodhue, J. Li, K. J. Linden, and W. E. Nixon, "Prospects for quantum cascade lasers as transmitters and local oscillators in coherent terahertz transmitter/receiver systems," Proc. SPIE **7215**, 72150C, (2009).
8. A. Baryshev, J. N. Hovenier, A. J. L. Adam, I. Kaalynas, J. R. Gao, T. O. Klaassen, B. S. Williams, S. Kumar, Q. Hu, and J. L. Reno, "Phase locking and spectral linewidth of a two-mode terahertz quantum cascade laser," Appl. Phys. Lett. **89**, 031115 (2006).
9. A. L. Betz, R.T. Boreiko, B. S. Williams, S. Kumar, Q. Hu, and J. L. Reno, "Frequency and phase-lock control of a 3 THz quantum cascade laser," Opt. Lett. **30**, 1837-1839 (2005).
10. D. Rabanus, U. U. Graf, M. Philipp, O. Ricken, J. Stutzki, B. Vowinkel, M. C. Wiedner, C. Walther, M. Fischer, and J. Faist, "Phase locking of a 1.5 Terahertz quantum cascade laser and use as a local oscillator in a heterodyne HEB receiver," Opt. Express **17**, 1159-1168 (2009).
11. A. A. Danylov, J. Waldman, T. M. Goyette, A. J. Gatesman, R. H. Giles, J. Li, W. D. Goodhue, K. J. Linden, and W. E. Nixon, "Terahertz sideband-tuned quantum cascade laser radiation," Opt. Express **16**, 5171-5180 (2008).
12. A. A. Danylov, J. Waldman, T. M. Goyette, A. J. Gatesman, R. H. Giles, K. J. Linden, W. R. Neal, W. E. Nixon, M. C. Wanke, and J. L. Reno, "Transformation of the multimode terahertz quantum cascade laser beam into a Gaussian, using a hollow dielectric waveguide," Appl. Opt. **46**, 5051-5055 (2007).

#108334 - $15.00 USD Received 4 Mar 2009; revised 15 Apr 2009; accepted 19 Apr 2009; published 22 Apr 2009

13. F. Bielsa, A. Douillet, T. Valenzuela, J.-P. Karr, and L. Hilico, "Narrow-line phase-locked quntum cascade laser in the 9.2 μm range," Opt. Lett. **32**, (2007).
14. D. W. Allan, "Statistics of atomic frequency standards," Proc. IEEE **54**, 221-230 (1978).
15. J. Rutman, "Characterization of phase and frequency instabilities in precision frequency sources: fifteen years of progress," Proc. IEEE **66**, 1048-1075 (1978).
16. G. Rau, R. Schieder, and B. Vowinkel, "Characterization and measurement of radiometer stability," Eur. Micro. Conf. 14th, 248 – 253 (1984).

1. Introduction

THz quantum cascade lasers [1] (TQCL) are a fast growing field with many potential applications. Progress has been made demonstrating a TQCL with high emission power [2], improved efficiency [3], low frequency operation [4], and high-temperature operation (178 K) [5]. For use in heterodyne receivers, particularly where coherent detection is required [6,7], the TQCL must be frequency stable over a long period of time (hours). Increased frequency stability improves system sensitivity and allows a number of high-resolution techniques to be implemented, which rely on stable phase measurements. For example, a range-resolving monostatic radar receiver suffers a phase error $\Delta\phi = 360(2R)\Delta\nu/c$ from a target at a distance R, due to a transmitter frequency shift, Δν. Thus, for short range (R ≤ 30 m) THz transceiver applications frequency stability of 50 kHz or better is required to achieve adequate phase stability. It has been already demonstrated that the inherent linewidth of a TQCL is extremely narrow [8], on the order of kHz or less, thus the crucial issue is stabilization of the TQCL frequency. This paper describes the details of stabilizing a TQCL to the kilohertz level.

A free-running TQCL's frequency varies with temperature fluctuations and power supply current noise through the active medium's index of refraction temperature dependence. With a conventional power supply (typically mA of noise) a TQCL's linewidth is several MHz wide, when measured over a time scale of seconds. In order to reduce the linewidth to the kHz level, the laser current source must have a noise level on the order of microamps (based on our measured current tunability of 6 MHz/mA). Such low noise, high current power supplies are not readily available. Additionally, temperature fluctuations have to be removed because of the TQCL's temperature sensitivity (100-200 MHz/K). Laser frequency stabilization to an external frequency reference can simultaneously reduce both current and temperature instabilities. Two possible compact frequency locking techniques involve using a molecular absorption resonance or the harmonic of an ultra-stable microwave source, but neither technique has yet been demonstrated. Instead, other complex THz sources, which have greater stability than the TQCL, have been used to demonstrate locking. Active stabilization was first demonstrated by Betz, et. al. [9], who achieved a 65 kHz full width at half maximum (FWHM) linewidth for a 3.06 TQCL, by locking to the 3.106 THz line of a CO_2 optically pumped laser (OPL). They attributed the rather large residual linewidth to the 10 kHz bandwidth limit of the feedback loop. Very recently, Rabanus, et. al. [10], achieved a much-improved 100 Hz linewidth by phase-locking a 1.5 THz QCL to a microwave-driven, harmonically generated THz source operating at 1499.3 GHz. However, data on the long-term stability of the lock circuit were not provided.

In this paper, we re-examine the issue of locking a TQCL to an OPL. Betz et. al. [9] used a source locking frequency counter (EIP 575) in their stabilization circuit. The EIP 575 is a microprocessor-based instrument with a sequence of pre-programmed operations designed to phase lock an external frequency to an internal, stable, and settable source. The "black box" nature of its operation limits remediation efforts in cases where phase locking fails. At the Submillimeter-Wave Technology Laboratory (STL), after failing to lock an OPL-QCL microwave beat frequency with this instrument, a more controllable, analog, frequency-locking approach was adopted to better understand the sources of noise.

2. Frequency locking technique

The QCL (2.408 THz, 1 mW of maximum optical power) was grown by UMass Lowell's Photonics Center, processed by Spire Corporation, and fully characterized by STL. The

#108334 - $15.00 USD Received 4 Mar 2009; revised 15 Apr 2009; accepted 19 Apr 2009; published 22 Apr 2009

details can be found in Ref. 11, 12. The TQCL was based on a single surface plasmon waveguide and had a 4 mm cavity length and a 100 μm waveguide ridge width. The laser in the CW mode emitted radiation primarily in a single-longitudinal mode (SLM) up to a bias voltage of 3.7 V and a multi-lodgitudinal mode (MLM) at higher voltages. It was mounted in a liquid-helium (LHe) dewar to keep the ambient device temperature at about 5 K. A hollow dielectric Pyrex tube of 30 mm length and 1.5 mm inner diameter was used as a mode filter to significantly improve the laser radiation transverse mode content to a near-Gaussian beam profile [12]. The TQCL was operated at 3.6 V (478 mA), approximately 0.2 V above threshold, to maintain the laser output to a single-longitudinal mode. The laser was driven by a 6 V battery through a 15 Ω potentiometer. A very stable CO_2 OPL was used as the reference source, which had a linewidth of 20-30 kHz due to mechanical and acoustic-induced laser cavity perturbations.

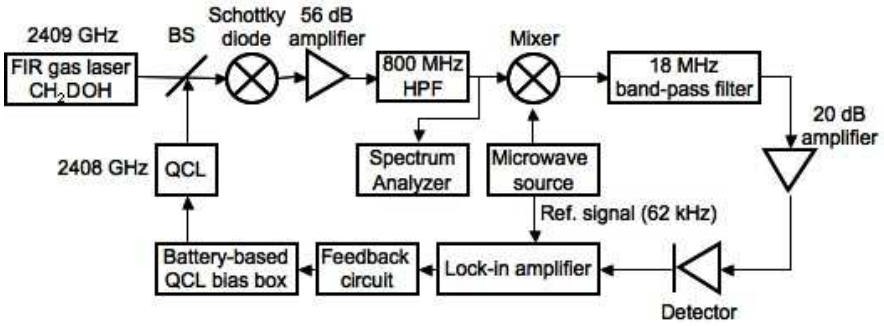

Fig. 1. Circuit configuration used in frequency locking the TQCL to the OPL. The modulated microwave source and bandpass filter provided an error signal that stabilized the intermediate frequency (IF), ($\nu_{QCL}-\nu_{OPL}$), and locked the quantum cascade laser to the OPL reference source.

The experimental setup is shown in Fig. 1. The CW free-running TQCL was mixed with the CW OPL, which lased on the 2409.293 GHz line of CH_2DOH. The TQCL radiation was collimated with an off-axis parabolic (OAP) mirror and, after combining with the reference radiation, focused with a second OAP onto the antenna of a whisker-contacted, corner-reflector-mounted Schottky barrier diode (SD) type 1T17, made by University of Virginia. The powers of the TQCL and the gas laser incident on the SD were about 300 μW and 3 mW, respectively. The TQCL frequency was approximately 1 GHz below the frequency of the gas laser. The GHz IF signal was amplified (56 dB), high-pass-filtered, and downconverted to 18 MHz with a microwave mixer and synthesizer source. The TQCL spectral properties were determined by analyzing the GHz IF signal with a spectrum analyzer. The 18 MHz signal was amplified (20 dB) and passed through a nominal 400 kHz (-3 dB) wide RF bandpass filter (BPF) centered at 18 MHz. The measured transmission spectrum of the BPF, shown in Fig. 2, has a FWHM of 610 kHz.

The synthesizer signal was sinusoidally frequency modulated at 62 kHz with a modulation depth of 500 kHz, and the 62 kHz modulation frequency was used as a reference signal for a lock-in amplifier (LIA), whose input was the RF-rectified 18 MHz signal. The lock-in output at the reference frequency is the first derivative of the bandpass signal which, fed back through the feedback circuit box to the QCL bias circuit at the proper gain setting and lock-in time constant, locked the frequency, $\Delta\nu = (\nu_{OPL} - \nu_{QCL})$ to the synthesizer signal. A 1 kHz bandwidth of the feedback loop was determined by the optimized LIA time constant of 1 ms.

#108334 - $15.00 USD Received 4 Mar 2009; revised 15 Apr 2009; accepted 19 Apr 2009; published 22 Apr 2009

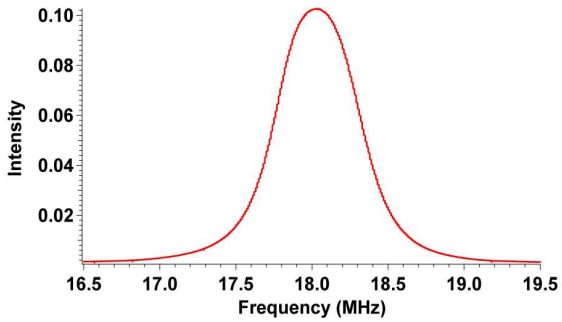

Fig. 2. Bandpass filter transmission spectrum with 610 kHz FWHM.

The feedback circuit is shown in Fig. 3. Proportional and integral feedback stages with independent and adjustable gain controls can be seen in the diagram. The fast frequency fluctuations were corrected by the proportional part of the circuit. The integrator (0.75 s time constant), based on an operational amplifier (OA), was designed to remove a very slow frequency drift. The feedback loop gains were adjusted by two 100 kΩ variable resistors. To correct the error signal polarity change produced by the integrator, an inverting amplifier with a gain of one was added to the integral part of the circuit. Both OAs were fed by 12 V batteries.

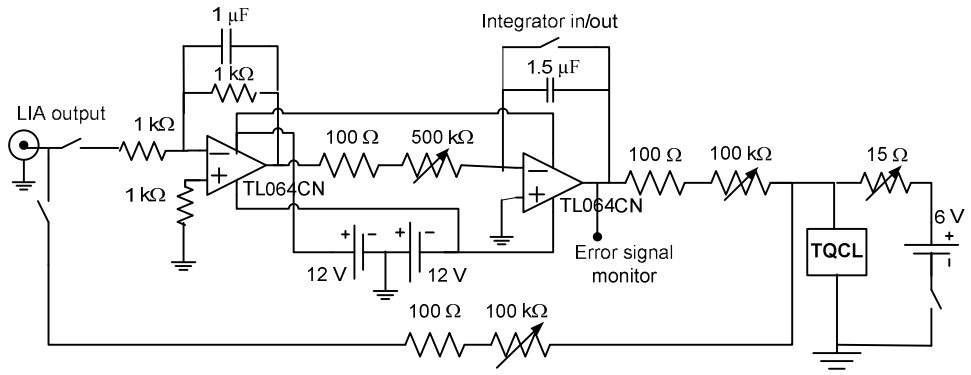

Fig. 3. The electronic feedback loop.

3. Stability results

The main results of the paper are shown in Figs. 4(a) and 4(b), where the locked spectra of ($\nu_{OPL} - \nu_{QCL}$) with 3-4 kHz linewidth (FWHM), taken over a frequency sweep duration of 60 seconds, are presented. To indicate a narrowing from 200 kHz to 3-4 kHz for the optimum parameters of the feedback circuit, an unlocked spectrum with a sweep time of 5 seconds is shown in Fig. 4(c).

#108334 - $15.00 USD Received 4 Mar 2009; revised 15 Apr 2009; accepted 19 Apr 2009; published 22 Apr 2009

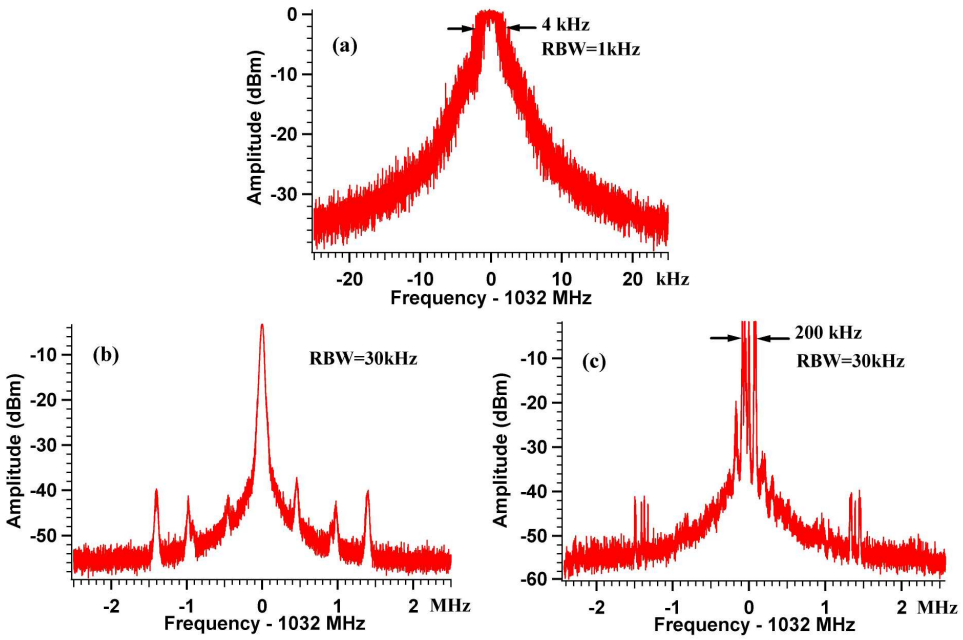

Fig. 4. Frequency spectra of (ν_{QCL}-ν_{OPL}) (RBW stands for a resolution bandwidth): (a) and (b) under locked conditions with 60 s scan time (4 kHz FWHM), (c) 5 sec scan with free-running QCL (200 kHz FWHM).

In principle, $\Delta\nu = (\nu_{OPL} - \nu_{QCL})$ can be more stable than the reference frequency, ν_{OPL}, if the feedback loop is sufficiently agile to adjust ν_{QCL} to correct for the jitter of ν_{OPL}, while simultaneously correcting for current fluctuations in the battery-driven QCL bias circuit. The measured linewidth, $\Delta\nu$ = 4 kHz, is narrower than the OPL reference, $\Delta\nu_{OPL}$, by a factor of 5, showing that the lock circuit is in great measure tracking the OPL frequency jitter. A similar spectral feature transferring effect can be found in Ref. 13, where a 9.2 μm QCL was phase-locked to a CO_2 laser line. Using two identical BPFs in series (450 kHz FWHM) instead of one did not reduce the beat frequency linewidth any further. Thus, we have shown that a 1 MHz feedback loop bandwidth is not required to reduce a TQCL linewidth to the kHz level, as assumed in Ref. 9.

The subsidiary peaks (420 kHz, 980 kHz, 1.4 MHz offset) in the beat spectrum shown in Fig. 4(b) have not been clearly identified. Beating of secondary transverse modes of the OPL, which was over-moded due to the large tube diameter for this wavelength, with the single mode of the QCL is the probable source of the three offset beat signals.

The locked spectrum with 50 ms sweep time averaged over 100 sweeps is presented in Fig. 5. The narrower linewidth of the fast-sweep, multiply-averaged spectrum, as compared with the slower single-sweep, Fig. 4(a), implies that the feedback circuit controls the frequency drift in $\Delta\nu$ better than it does the jitter. While reduced 50-fold by the lock, the jitter is still evident in the flat peak of the spectrum of Fig. 4(a). Further adjustments of the feedback circuit and a more stable reference source may enable TQCL frequency stabilization to a (-3 dB) linewidth of 1 kHz or less, with the frequency-locking approach described here.

#108334 - $15.00 USD Received 4 Mar 2009; revised 15 Apr 2009; accepted 19 Apr 2009; published 22 Apr 2009

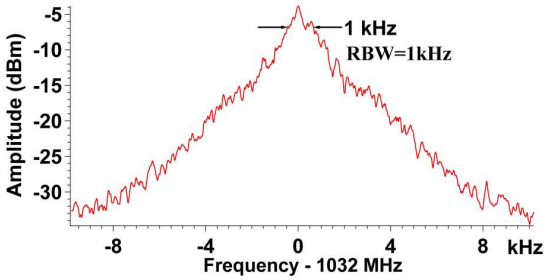

Fig. 5. Frequency spectrum (1 kHz FWHM) under locked condition with 50 ms scan time (the spectrum was averaged over 100 scans).

The unlocked TQCL experienced, in addition to a short-term frequency jitter, a long-term frequency drift with a relatively constant rate of approximately +4.8 kHz/sec. The drift is shown in Fig. 6(a), where the beat frequency deviation was recorded with time. The slow and constant temperature drift of the 15 Ω potentiometer was the source of this effect. When the TQCL was stabilized with only a proportional part of the feedback circuit, the beat frequency linewidth and frequency drift was reduced to 3-4 kHz and 50 Hz/sec, respectively. Employment of the integrator in the frequency locking process did not reduce the linewidth any further, but did help to substantially reduce the drift to a value of 0.13 Hz/sec. This can be seen in Fig. 6(b), where a typical time-domain record of the beat frequency for a 45-min period is presented. The time interval between readings was 2 seconds. After about 2100 seconds the TQCL dewar ran out of LHe and, as a result, frequency drift increased. The maximum frequency excursion was only about 200 Hz within a 40 minute time frame.

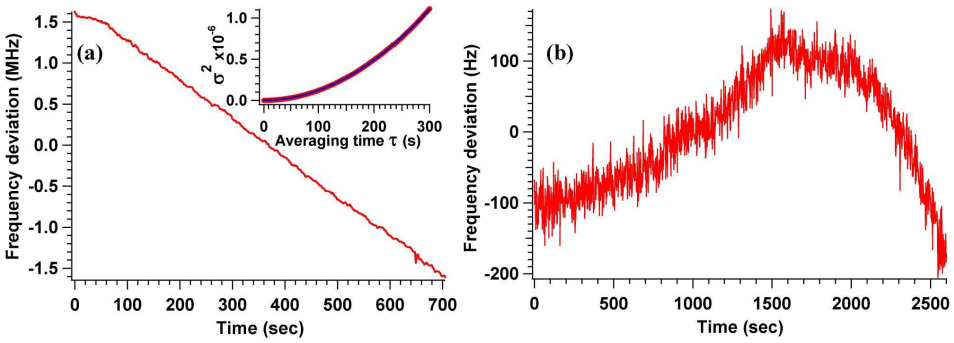

Fig. 6. Beat frequency fluctuation recorded (2 sec/point) during: (a) a 12-min time interval of the free-running TQCL, (Inset: Allan variance plot of the unlocked laser discussed in Sect.4), (b) a 45-min time interval of the locked TQCL.

The largest correction signal that the integrator can produce was 12 V. By the time the TQCL dewar emptied, the error signal monitor (Fig. 3) indicated only 2 V. Thus, the frequency locking time was restricted only by the dewar's LHe capacity and can be extended significantly by using a different TQCL cooling system.

4. Time domain analysis

In order to quantitatively evaluate the TQCL and OPL beat frequency stability, a two-sample Allan variance was calculated for averaging times between 2 s and 300 s. The Allan variance is defined by [14,15]:

$$\sigma^2(2,\tau)=\frac{1}{2(m-1)\nu_0^2}\sum_{i=1}^{m-1}\left(\overline{\nu}_{i+1}-\overline{\nu}_i\right)^2, \qquad (1)$$

#108334 - $15.00 USD Received 4 Mar 2009; revised 15 Apr 2009; accepted 19 Apr 2009; published 22 Apr 2009

where m is the number of measurements of $\overline{\nu}_i$, each averaged over a τ time interval (assuming zero dead time) and ν_0 is the mean frequency. The square root of Allan variance is called Allan deviation (AD). Fig. 7(a) shows Allan variance calculated using frequency fluctuation data from 2–2100 s time interval (before the TQCL temperature increased due to lack of LHe in the dewar). Increasing the averaging time improves the beat frequency stability by averaging noise. The Allan deviation reaches its minimum value of $\sigma(2,26)=7.1\cdot10^{-9}$ at the optimum averaging time of 26 s. After this point longer averaging times reduce the level of stability. Plotting log (σ^2) versus log (τ) allows identification of the noise types [14,16]. As can be seen from Fig. 7(b), the curve has a slope of about -1 in region I for short integration times up to τ = 26 s (log τ =1.4), indicating that white noise was dominant in this section. Flicker noise (1/f) is responsible for the flat minimum section in region II from τ = 26 s to 40 s (1.4 < log (τ) < 1.6). After this point low-frequency random-walk and flicker-walk noises (drifts) drive the curve up with a slope of ~ 1.8 (section III). Environmental perturbations like mechanical vibrations and temperature fluctuations are responsible for this type of noise.

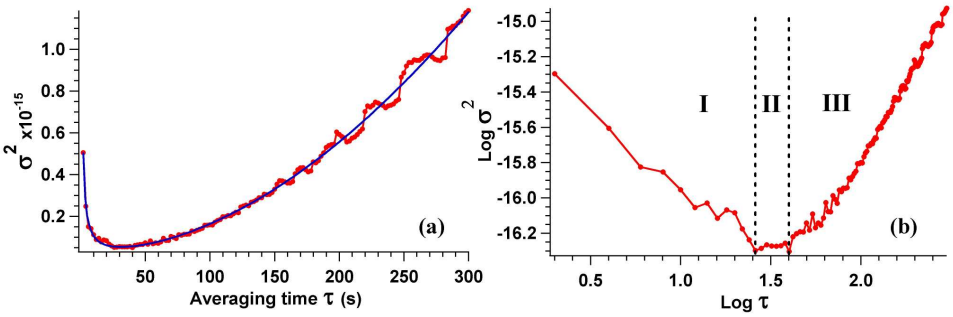

Fig. 7. (a) Allan variance σ^2 (red line) plot and its fit curve (blue line) for the locked TQCL, (b) Log σ^2 vs Log τ. Region I (slope -1) is dominated by white noise, region II (slope 0) is dominated by flicker noise, and region III (fractional slope of 1.8) is dominated by a noise type positioned in power law model between random-walk (slope 1) and flicker-walk (slope 2) noises.

Frequency noise consists of white (W ~ f^0), flicker (F ~ f^{-1}), random-walk (RW ~ f^{-2}), and flicker-walk (FW ~ f^{-3}) noise. The Allan variance in our case can be represented by the expression [16]:

$$\sigma^2(2,\tau)=a_{FW}\tau^2+a_{RW}\tau^{1.8}+a_F+a_W/\tau\,. \tag{2}$$

A fitting routine to our data (Fig. 7(a)) gives the following noise level constants:

$$a_{FW}=5\times10^{-21}, a_{RW}=2.49\times10^{-20}, a_F=4.2\times10^{-18}, a_W=9.97\times10^{-16}.$$

White noise is the dominant noise with some contribution from flicker and some weak frequency drift expressed by FW and RW noise. However, since we are analyzing the beat signal between the OPL and TQCL, we cannot identify the source (the OPL or the TQCL) of the noise. To make a comparison between locked and unlocked beat frequency stability, Allan variance of the free-running TQCL was calculated and shown in the inset of Fig. 6(a). It can be described by the formula

$$\sigma^2(2,\tau)=b_{FW}\tau^2 \tag{3}$$

where the fitting constant is

#108334 - $15.00 USD Received 4 Mar 2009; revised 15 Apr 2009; accepted 19 Apr 2009; published 22 Apr 2009

$$b_{FW} = 1.228 \times 10^{-11}.$$

The fit between the measured data is perfect. Flicker-walk noise is the only noise that can be identified here as it should be since there is a very strong frequency drift of the unlocked laser (Fig. 6(a)). By comparing the noise level coefficients we conclude that significant noise reduction has been achieved.

6. Conclusion

It has been demonstrated that the THz QCL can be frequency locked and stabilized to that of a THz reference source using downconversion, comparison to a microwave synthesizer signal, RF filtering, and a relatively slow (τ ~ 1ms) proportional and integral analog feedback circuit. The frequency stability of the beat signal, $\Delta\nu$, based on the square root of Allan variance, was estimated (7.1×10^{-9} at the optimum averaging time of 26 sec). The long-term stability of the OPL and the proportional/integral feedback circuit maintained the 3-4 kHz linewidth for a time of 45 minutes, limited only by the capacity of the LHe dewar. THz QCLs with achieved frequency stability can be used as transmitters in short-range coherent transceivers and many other applications.

Acknowledgments

We are grateful to K. Linden from Spire Corporation for fabricating the THz QCL for this experiment. This work was supported by the U.S. Army National Ground Intelligence Center.

#108334 - $15.00 USD Received 4 Mar 2009; revised 15 Apr 2009; accepted 19 Apr 2009; published 22 Apr 2009